AIAA JOURNAL
Vol. 49, No. 6, June 2011

Accuracy of Direct Skin-Friction Measurements in High-Enthalpy Supersonic Flows

Taira Tsuru*
Tokyo Institute of Technology, Kanagawa 226-8502, Japan
Sadatake Tomioka†
Japan Aerospace Exploration Agency, Miyagi 981-1525, Japan
and
Hiroyuki Yamasaki‡
Tokyo Institute of Technology, Kanagawa 226-8502, Japan

DOI: 10.2514/1.J050691

Measurement of skin friction and a survey of airflow momentum were conducted in a rectangular straight duct with airflow Mach number, unit Reynolds number, and stagnation enthalpy at the nozzle exit of 2.5, 2.7 × 10^7 m^{-1}, and 1.1 MJ/kg, respectively. Skin fiction was measured by a direct skin-friction sensor at the test section that was connected to the duct exit, with the state of airflow there also being surveyed. From the result of the measurement and survey at two streamwise locations with different lengths, mean skin friction was calculated by two different and independent methods. The mean skin friction calculated by the directly measured skin friction was compared with that calculated by the momentum conservation law in order to examine the accuracy of direct skin-friction measurement. The accuracy of skin-friction measurement using the direct skin-friction sensor in the test was found to be ±5% (root-sum-square value).

Nomenclature

A	=	cross-sectional area for calculation (30 mm × 32 mm)
C_f	=	local skin-friction coefficient
q	=	dynamic pressure, $\rho U_e^2/2$
Re_u	=	unit Reynolds number, U_e/ν
S	=	unit wetted area between two duct exits (30 mm × 400 mm × 2)
T	=	temperature
U	=	velocity
X	=	streamwise location from the nozzle throat
Y	=	lateral location from the inner wall surface of the duct
Z	=	spanwise location from the duct center
ε	=	error
ν	=	coefficient of kinematic viscosity
ρ	=	density
τ_w	=	wall skin friction
–	=	mean value of variables

Subscripts

d	=	straight duct
e	=	conditions external to boundary layer
t	=	stagnation conditions
w	=	conditions at wall
0	=	air heater conditions
1, 2	=	duct exit number

Received 16 June 2010; revision received 2 November 2010; accepted for publication 20 January 2011.

*Postgraduate Student, Department of Energy Sciences, 4259 Nagatsuda, Midori-ku, Yokohama.
†Senior Researcher, Kakuda Space Center, Advanced Technology Research Group, 1 Koganezawa, Kimigaya, Kakuda. Senior Member AIAA.
‡Professor, Department of Energy Sciences, 4259 Nagatsuda, Midori-ku, Yokohama. Member AIAA.

I. Introduction

FRICTION in supersonic flow is an important factor in aerospace engineering. For instance, regarding the previous results at the Japan Aerospace Exploration Agency's Kakuda Space Center under M6 and M8 flight conditions, it was evaluated by one-dimensional calculation that the wall skin friction corresponded to about 80–90% of the whole drag that acted on the tested hypersonic airbreathing engine model [1,2]. Thus, a small change in C_f results in a substantial increase in the friction drag when the engine is operated at hypersonic speed [3]. Therefore, an accurate evaluation of the skin friction is important for analysis and prediction of drag force that acts on the engine.

There have been several reports on direct measurement of skin friction using a direct skin-friction sensor in a high-enthalpy flowfield, for example, the internal flow of a hypersonic airbreathing engine combustor [4–6]. In addition, when evaluating a method of predicting C_f in the turbulent boundary-layer flow, for example, the measured values by direct skin-friction measurements were compared. The direct skin-friction measurements, in this way, have been used under such condition as a complicated flowfield with turbulence and combustion.

There are two methods of direct measurement of skin friction: the compensating type (nulling type) and the noncompensating type (nonnulling type). Error sources analysis of direct skin-friction measurement has been conducted. For example, regarding systematic error sources, the effect of misalignment of the sensor setting on direct skin-friction measurement using a compensating-type sensor was examined in the condition of a supersonic flow with lower enthalpy [7]. In addition, in both cases of laminar channel flow and turbulent flow on an external flat plate, computational fluid dynamics has been used to examine the effects of geometric design and installation of a non-compensating-type direct skin-friction sensor on measurement [8,9].

While several research studies examining error sources of direct skin-friction measurement have been conducted as mentioned above, no tests examining the accuracy of directly measuring skin friction in a flowfield have been conducted so far. Therefore, first of all, accuracy (degree of certainty) of the direct skin-friction measurement should be verified by any other plausible methods with fewer assumptions in order to use it as a reliable tool of measuring skin friction. The objective of this research was to confirm the accuracy of

direct skin-friction measurement to evaluate skin friction with confidence.

In this study, skin friction was measured by a direct skin-friction sensor in a high-enthalpy flow of a rectangular straight duct with a constant cross-sectional area. Accuracy of the direct skin-friction measurements was confirmed by calculation of mean skin friction. The mean skin friction between two duct exits was obtained by measuring skin friction at each duct exit, and that mean skin-friction value was verified by that obtained by calculating the momentum at each duct exit by surveying the state of air flow at each duct exit (this verification approach was based on momentum conservation law).

II. Experimental Apparatus

A. Wall Skin-Friction Sensor

There are various methods of evaluating the wall skin friction, for example, use of a Stanton tube and a Preston tube. As for optical methods, Moiré fringe analysis observes the interference fringe of the oil on the surface that shear stresses are acting on. However, all the above techniques have some assumptions regarding flow. For example, when a Preston tube is used for evaluation of C_f using the velocity profile in the turbulent boundary layer (Clauser plot), flow should obey the law of wall, and there should be no pressure gradient. Unless the wall temperature is approaching the adiabatic wall temperature, good accuracy of C_f evaluation is not obtained [10]. When adapting the Moiré method, skin friction should not be changed during measurement and flow is two-dimensional flow, etc. [11]. However, there is little restriction on the use of direct measurement, and such measurement can sense unsteady change of skin friction in complex internal flow even in a hypersonic airbreathing combustor.

There are two types of direct measurement of wall friction. One is a method of compensating for the shear stress acting on the sensor head so as to balance the shear stress (nulling type). In this design, the floating head will not have a net deflection. The other type is a method of noncompensating for shear stress acting on the sensor head. In this design, the floating head will be deflected by shear. Regarding structure, in the nulling design, a restoring force equal to the shear force is applied through complex mechanical devices. Such configurations are very delicate and have a slow response time. In this research, a non-compensating-type (non-nulling-type) sensor was used because it had a fast response and was easy to fabricate compared with the compensating-type sensor [7].

A schematic diagram of the skin-friction sensor used in this research is shown in Fig. 1. This type of sensor was invented and used by researchers at the Virginia Polytechnic Institute and State University [7]. A feature of this wall friction sensor is that it uses the cantilever beam. The head of the beam is made of SUS304 steel, the same material as that of the inner wall of the test section, and the beam used is material of suitable strength and elasticity. Two pairs of film strain gauges (four gauges in total) are placed orthogonally on the surface of the end of the beam. Therefore, this sensor can measure two orthogonal components of the surface shear force.

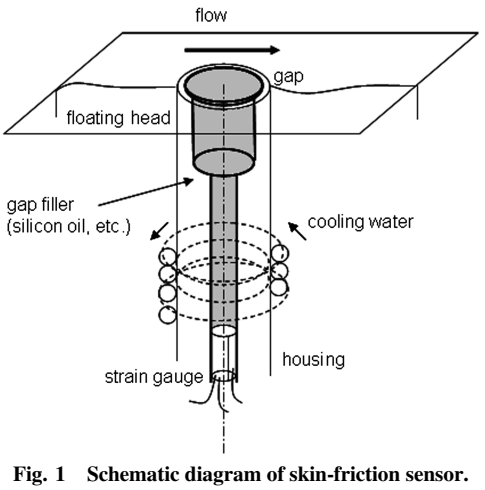

Fig. 1 Schematic diagram of skin-friction sensor.

The skin-friction sensor system in this research uses a Wheatstone bridge for output against shear stress and can measure shear stress ranging from about 14 to 1500 Pa. Moreover, the sensor beam is surrounded by a sufficient amount of silicon oil, which works as a thermal insulator of the strain gauge and a vibration absorption agent for the beam. The oil also eases the effect of the pressure gradient around the sensor head. That is, the oil provides a continuous surface to the flow and prevents flow into and out of the gap. That prevents force generated by the difference of pressure around the lip of the sensor head [3].

The sensor head was flush-mounted so as not to protrude into the flow as its protrusion would generate error of skin-friction measurement. The diameter of sensor was 9.5 mm and the sensor head was surrounded by silicon oil on the wall surface. This oil made a continuous surface and flow did not enter the sensor. Thus, only the surface of the sensor head was exposed to flow and shear worked on it.

During the test time (2.4 s) while wall skin friction and wall static pressure were being monitored (the sampling rate was 200 Hz), the fast Fourier transformation (FFT) analysis using a Hamming window (window function) of those waves was conducted. No excited peak of the spectrum that was thought to be natural vibration frequency of the skin-friction sensor was detected. There was no phase shift because the sine component was zero from the result of the FFT with regard to both waves of wall pressure and skin-friction output. The response of the skin-friction sensor was thought to be sufficiently fast, because there was no phase shift compared with the result of the FFT analysis of wall pressure wave. (The response time of wall pressure sensor using a strain gauge is a few milliseconds.)

As described above, the advantage of using a direct skin-friction sensor is that it can sense even unsteady change of skin friction during measurement without interfering with the flow, which otherwise would not be possible.

The direct skin-friction sensor is tolerable to heat with cooling by the oil and it is a simple mechanism to fabricate. It is easy to deal with the heat effect without interfering with the flow, which is difficult with other options.

The estimated systematic error of this skin-friction sensor is $\pm 2.2\%$ (root-sum-square value) following the uncertainty methods [12]. The estimated sources of the error are shown in Table 1.

B. Wind-Tunnel Facility and Test Apparatus

The rectangular straight duct whose length was varied was directly connected to a blowdown wind tunnel. A vitiated air heater was used to generate high-enthalpy airflow supplied into the straight duct. H_2, O_2, and air were supplied into the vitiated air heater to obtain test gas with its mole fraction of oxygen being equal to that of standard air.

The products of vitiated air were N_2, O_2 and H_2O. (CO_2 was almost 0 as well as standard air) Their mole ratio was 69, 21, and 9%, respectively, as calculated by NASA CEA2 program [13]. The specific heat ratio of the vitiated air in the core flow was 1.38 when the condition of T was 430 K (static temperature) and P was 90 kPa (wall pressure) at the test section. (That of the standard air was 1.39.) At the near wall, T was about 500 K, then the specific heat ratios of the vitiated air was 1.37 and that of the standard air was 1.39.

As to calculation of momentum, the effect of vitiated air (including H_2O) might have had an effect on the composition of the flow state,

Table 1 Estimated sources of systematic error

Source	Value
Axial rotation	$\pm 1.5\%$
Zero drift	$\pm 0.1\%$
Gap to lip ratio error	$\pm 0.5\%$
Protrusion error	$\pm 1.0\%$
Temperature drift during testing	$\pm 1.0\%$
Truncation (data reduction)	$\pm 0.5\%$

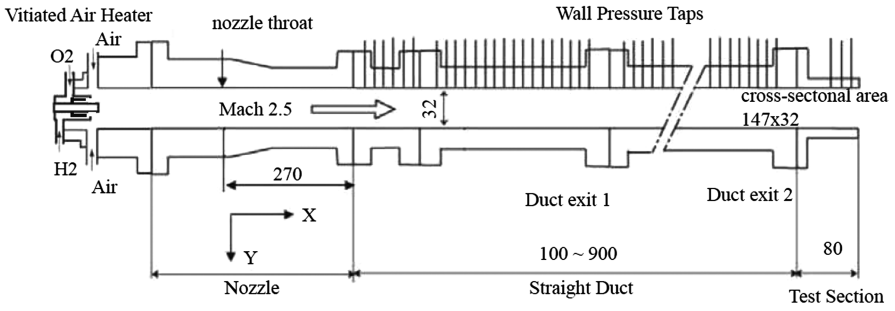

Fig. 2 Schematic diagram of the facility setup.

but did not affect comparing momentum calculation of each duct exit because the mean skin friction was calculated by difference of momentum.

Total temperature of the test gas ($T_{t,0}$) was 1000 K ± 5% and total pressure ($P_{t,0}$) was 1.5 MPa ± 4%. The standard deviation of $T_{t,0}$ and $P_{t,0}$ for all runs were ±1% and less than ±0.1%, respectively. The test gas was accelerated by a two-dimensional heat-sink nozzle to Mach 2.5. The unit Reynolds number at the exit of the nozzle was 2.7×10^7 m^{-1}. At the nozzle exit, the boundary layer was thought to be fully developed turbulent flow.

A schematic diagram of the facility setup to examine the accuracy of the skin-friction measurement is shown in Fig. 2. The facility nozzle was directly connected to the vitiated air heater. The straight duct (100–900 mm) was connected to the nozzle. The test section (80 mm) was connected to the straight duct. The cross-sectional area of the test section (80 mm) and the straight duct (100–900 mm) was 147 mm × 32 mm.

A schematic diagram of the test section is shown in Fig. 3. The test section was installed at the exit of the straight duct. The skin-friction sensor was mounted flush to the internal surface of the test section. The diameter of the skin-friction sensor head was 9.5 mm and the gap length was 0.15 mm. Chromel-alumel thermocouples were also installed on the wall of test section and in the housing of the skin-friction sensor. The thermocouples monitored T_w of the test section and the oil temperature around the strain gauge in the skin-friction sensor. The heat flux sensor was installed on the test section wall surface of the opposite side on which the skin-friction sensor was installed in order to monitor heat flux on the wall surface during the test.

C. Two Methods of Evaluating Mean Skin Friction

The test section was installed at the exit of the straight duct and the wall skin friction was measured there. Skin-friction force was assumed to be distributed logarithmic with the X in the streamwise direction because C_f is the roughly approximated power or logarithmic function of Re_x in the fully developed turbulent boundary layer with $Re_x > 10^7$. The mean wall skin friction between the two exits was calculated directly from the skin-friction measurement with the following Eq. (1):

$$\overline{\tau_{w1-2}} = \left(\int_1^2 \tau_w \mathrm{d}X \right) \Big/ (X_2 - X_1) \tag{1}$$

On the other hand, the state of the flow was also surveyed. The total temperature and pitot pressure were measured at each duct exit, and the momentum for each unit cross-sectional area (30 mm × 32 mm) at each exit location was calculated using the NASA-CEA2 equilibrium calculation code [13]. For this calculation of momentum using the measured total temperature of the flow, heat flux onto the wall surface was not taken into account in calculation of velocity. The velocity profile of the boundary layer can also calculated by the Crocco–Busemann relation between T, T_w, and u [14,15]. In the present study, wall temperature and heat flux were also measured during the test. The wall temperature increased at a depth of 0.5 mm from the wall surface and the heat flux (0.79 MW/m^2) was steady during the test. Velocity was calculated by the Crocco–Busemann relation using an average value of T_w (about 470 K) during the test. The difference between the velocity calculated by the Crocco–Busemann relation and that calculated using the measured total temperature was less than 1% in the experimental condition.

As shown by the momentum distributions in Sec. III, no abrupt change of momentum thought to be caused by shock was detected.

The Mach number at the duct exit was also calculated when calculating momentum. From the distribution of the Mach number, no abrupt change caused by shock was detected. The typical Mach number of the core flow was 2.5 at the duct exits and decreased gradually in the boundary layer.

The mean wall skin friction between the two exits was calculated with the following Eq. (2):

$$\overline{\tau_{w1-2}} = \left(\int \rho_1 u_1^2 \, \mathrm{d}A - \int \rho_2 u_2^2 \, \mathrm{d}A \right) \Big/ S \tag{2}$$

This is called the momentum-loss method in this study and a schematic diagram of the unit calculation volume is shown in Fig. 4. Then the error of the measurement was examined by comparing mean skin frictions calculated by both of the methods.

D. Measurements and Data Reduction

Pressure taps with a diameter of 1.0 mm were attached to the side walls and the wall of the test section around the skin-friction sensor. Wall pressure distribution was measured in the streamwise direction by two mechanical pressure scanners (Scanni-valve Company model J; range: 0–700 kPa; error: ±0.2% full scale). To mitigate the run-to-run deviation of the test conditions, the measured pressure was

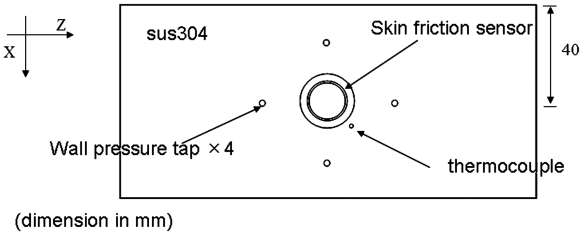

Fig. 3 Schematic diagram of the test section.

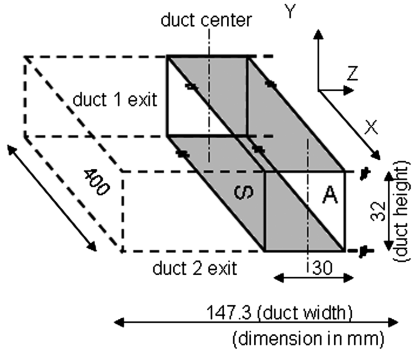

Fig. 4 Unit volume for calculation.

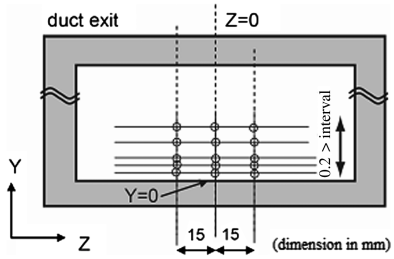

Fig. 5 Schematic of pitot pressure and total temperature measurement positions.

Table 2 Test conditions

Condition	Value
$T_{t,0}$	1000 K
$P_{t,0}$	1.5 MPa
Mach number at the nozzle exit	2.5
Re_u	2.7×10^7 m^{-1}
Test-section distance from nozzle throat, X	770 mm (d_1), 1170 mm (d_2)

normalized with the total pressure of the airflow measured in the setting chamber.

Pitot pressure and total temperature measurement were conducted by probes at the straight duct exit to survey the state of airflow for calculating momentum of the flow as mentioned above. The interval of the measurement point in the Y direction was more than 0.2 mm. Measurement in the Y direction was conducted from the wall surface ($Y = 0$) to 16 mm by traversing the probes. At the duct 1 exit, for example, the height of the first point of measurement from the wall was 0.5 mm and at the same height, three points were measured in the Z direction. When the average value located at the same Y position was calculated, data at three points with identical Y ($Z = -15, 0$, and $+15$ mm) were adopted. For example, the mean values of momentum as in Sec. III were calculated in the same manner. A schematic of the measurement positions is shown in Fig. 5.

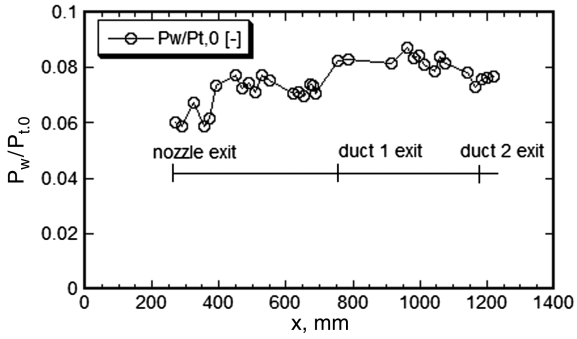

Fig. 6 Wall pressure distribution.

III. Results and Discussion

The test conditions are shown in Table 2. Wall pressure distribution is shown in Fig. 6. Wall pressure increased gradually in the streamwise direction. The total pressure decreased mainly due to skin friction and pressure gradient at each test section ($X = 770$ and 1170 mm) was negligible. Therefore, skin-friction measurement in this study was not affected by pressure gradient around the friction sensor head.

Typical records of skin friction are shown in Figs. 7a and 7b, with analysis time being set from 15–17.4 s (2.4 s). The output from the skin-friction sensor during the analysis time showed that the wall skin friction was steady.

The momentum distribution at each duct exit is shown in Figs. 8a and 8b. The momentum distributions of the mean value at the two duct exits ($X = 770$ and 1170 mm) are shown in Fig. 9. Dynamic pressure of the core flow at each duct exit was 408 kPa $\pm$ 2%, and the core of airflow existed even at 1170 mm from the nozzle throat. From those results, transportation of momentum in the Z direction only slightly occurred in the unit volume. Therefore, the momentum was thought to gradually decrease in the streamwise direction due to wall skin friction.

Comparison of mean skin friction is calculated by two different methods, as follows:

When calculated by direct measurement of skin friction, $\overline{\tau_{w1-2}} =$ 1072 Pa $\pm$ 5% (where $\overline{\tau_{wa-b}}$ is the mean skin friction between duct exit a and duct exit b, for example). The estimated relative error of the mean skin friction is estimated from the repeatability of $\pm$4.3% and systematic error of $\pm$2.2%. Skin-friction measurements were conducted three–four times at each duct exit. The measured value of standard deviation was within 1% for each measurement, and repeatability was calculated among them for each duct exit. The sources of error, $a \pm 4.3\%$ repeatability, was thought to be due to the manner of setting the sensor. The accuracy of mean skin friction by the measurements was $\pm 5\%$ $(\pm 4.3\%^2 + \pm 2.2\%^2)^{1/2}$ (root-sum-square value).

When calculated by momentum integration, $\overline{\tau_{w1-2}} = 1060$ Pa $\pm$ 10% (see the Appendix).

Systematic error of both methods was almost the same (about 2–3%), but the error from repeatability by direct skin-friction measurement was larger than that of the momentum-loss calculation. The difference between mean values of the two methods is thought to depend on the assumption of skin-friction force distribution between two duct exits. As to evaluation of mean skin friction, the accuracy of the momentum-loss method was better than that of the direct skin-friction measurement.

The range of mean skin-friction value calculated by direct skin-friction measurement included that by the momentum-loss method. Then the accuracy of direct skin-friction measurement was verified by the momentum-loss method. The repeatability of the measured skin-friction value was $\pm$4.3% (standard deviation) and the systematic error was $\pm$2.2%. The accuracy of direct measurement

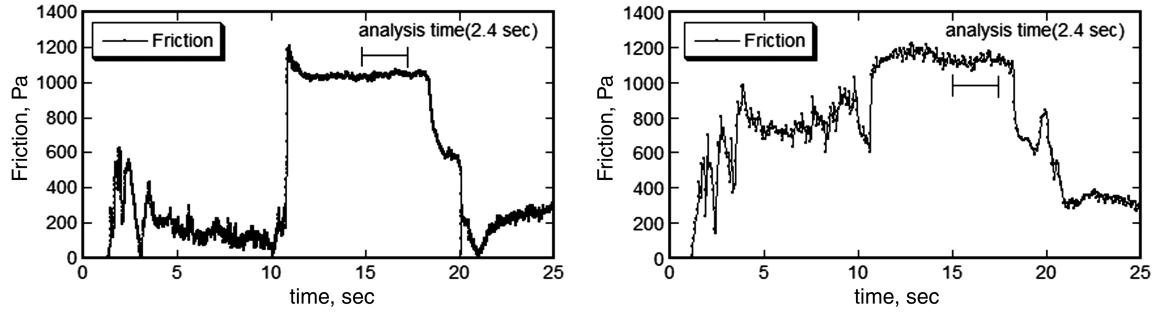

Fig. 7 Typical output of friction during test a) duct 1 exit b) duct 2 exit.

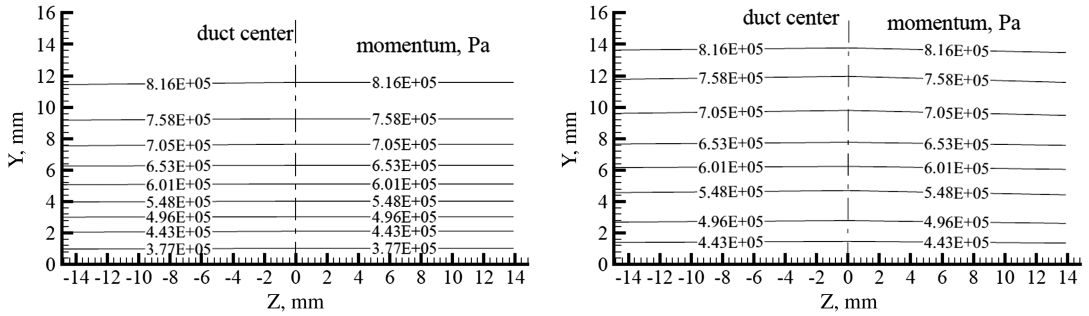

Fig. 8 Momentum distribution of a) duct 1 exit and b) duct 2 exit.

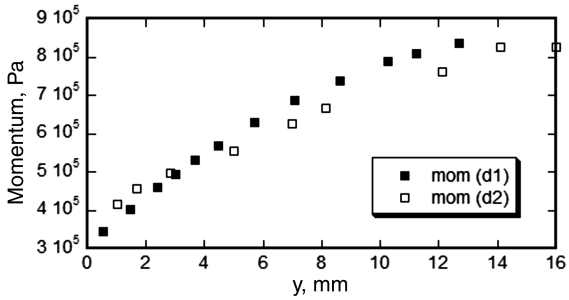

Fig. 9 Momentum distribution of duct exits (mean value).

using the skin-friction sensor in the test was found to be ±5% (root-sum-square value).

IV. Conclusions

Accuracy of the direct skin-friction measurements was examined by calculation of mean skin friction. The mean skin friction between two duct exits was obtained in two ways from the results of skin-friction measurement and survey of flow state at each duct exit. The range of the mean skin-friction value calculated by direct skin-friction measurement included that by the momentum-loss method. The accuracy of direct skin-friction measurement was verified by the momentum-loss method.

The repeatability of measured skin-friction value was ±4.3% (standard deviation) and the systematic error was ±2.2%. The accuracy of direct measurement using skin-friction sensor in the test was found to be ±5% (root-sum-square value). Therefore, the measured skin-friction by using the direct skin-friction sensor in this study had sufficient accuracy to be adopted as reliable data.

Appendix: Accuracy of Mean Skin Friction by Method of Momentum Integration

The momentum integration of a fixed unit cross section of each duct exit was calculated. The method of calculating the mean skin friction between each duct and sources of the error caused by this procedure are shown.

1) At duct exits 1 and 2, the repeatability of T/T_0 was ±0.2%.

2) The calculated momentum was ±0.2% by the equilibrium calculation with $T_{t,e}$, T_t, $P_{t,e}$, and P_t. Momentum integration was conducted for the unit cross-sectional area of each duct exit.

3) The mean skin friction between the two duct exits using momentum integration of item 2. The estimated error as to the calculated value of the mean skin friction became ±106 Pa, which was about ±10% of the mean skin friction, 1060 Pa.

References

[1] Mitani, T., Tomioka, S., Kanda, T., Chinzei, N., and Kouchi, T., "Scramjet Performance Achieved in Engine Tests from M4 to M8 Flight Conditions," 12th AIAA International Space Planes and Hypersonic Systems and Technology, AIAA Paper 2003-7009, Norfolk, VA, Dec. 2003.

[2] Flankl, F., and Voishel, V., "Turbulent Friction in the Boundary Layer of a Flat Plate in a Two-dimensional Compressible Flow at High Speeds," NACA TM 1053, 1943.

[3] Smith, T. B., and Schetz, J. A., "Direct Skin Friction Measurement in a Rocket-Based-Combined-Cycle Scramjet Combustor," 36th AIAA/ASME/SAE/ASEE Joint Propulsion Conference & Exhibit, AIAA Paper 2000-3724, Huntsville, AL, July 2000.

[4] DeTurris, D. J., and Schetz, J. A., "A Technique for Direct Measurement of Skin Friction in Supersonic Combustion flow," Virginia Polytechnic Institute and State University, Rept. VPI-AOE-196, Blacksburg, VA, Dec. 1992.

[5] Orth, R. C., Billig, F. S., and Gremleski, S. E., "Measurement Techniques for Supersonic Combustion Testing," *Symposium on Instrumentation for Airbreathing*, Monterey, CA, Sept. 1972, pp. 263–282.

[6] Stalker, R. J., Paull, A., Mee, D. J., Morgan, R. G., and Jacobs, P. A., "Scramjets and Shock Tunnels—The Queensland Experience," *Progress in Aerospace Sciences*, Vol. 41, 2005, pp. 471–513. doi:10.1016/j.paerosci.2005.08.002

[7] Schetz, J. A., "Direct Measurement of Skin Friction in Complex Flows Using Movable Wall Elements," 24th Aerodynamic Measurement Technology and Ground Testing Conference, AIAA Paper 2004-2112, Portland, OR, July 2004.

[8] Allen, J. M., "Improved Sensing Element for Skin-Friction Balance Measurement," *AIAA Journal*, Vol. 18, No. 11, Nov. 1980, pp. 1342–1345. doi:10.2514/3.50889

[9] MacLean, M., and Schetz, J. A., "Study of Internal Flow Effects on Direct Measurement Skin Friction Gages," 40th Aerospace Sciences Meeting and Exhibit, AIAA Paper 2002-0531, Reno, NV, Jan. 2002.

[10] Allen, J. M., "Use of Baronti-Libby Transformation and Preston Tube Calibrations to Determine Skin Friction from Turbulent Velocity Profiles," NASA TN D-4853, 1968.

[11] Kennelly, R. A., Jr., and Goodsell, A. M., "Skin Friction and Transition Location Measurements on Supersonic Transport Models," *9th International Symposium on Flow Visualization*, Edinburgh, Scotland, U.K., 2000.

[12] Figlioa, R. S., and Beasley, D. E., *Theory and Design for Mechanical Measurements*, 4th ed., Wiley, New York, 1995, pp. 171–210.

[13] Zehe, M. J., Gordon, S., and McBride, B. J., "CAP: A Computer Code for Generating Tabular Thermodynamic Functions from NASA Lewis Coefficients," NASA TP-2001-210959-REV1, 2002.

[14] White, F. M., *Viscous Fluid Flow*, 2nd ed, McGraw–Hill, Upper Saddle River, NJ, 1991, p. 546.

[15] Van Driest, E. R., "Turbulent Boundary Layer in Compressible Fluids," *Journal of the Aeronautical Sciences*, Vol. 18, No. 3, 1951, p. 150.

N. Chokani
Associate Editor